Microchimica Acta (2019) 186:662
https://doi.org/10.1007/s00604-019-3780-3

ORIGINAL PAPER

Click DNA cycling in combination with gold nanoparticles loaded with quadruplex DNA motifs enable sensitive electrochemical quantitation of the tuberculosis-associated biomarker CFP-10 in sputum

Jinlong Li[1] · Kai Hu[2] · Zhaoli Zhang[1] · Xiaoyan Teng[1] · Xia Zhang[3,4]

Received: 30 July 2019 / Accepted: 21 August 2019

Abstract

An electrochemical aptamer-based assay is described for the determination of CFP-10 which is an early secretary biomarker of *Mycobacterium tuberculosis*. CFP-10 is specifically captured by its aptamer and then induces a DNA cross-linking click reaction, the release of CFP-10, and an amplification cycle of repeated CFP-10 release. This mechanism (with dual amplification via DNA click and target release cycle) causes more and more CFP-10 Apt strands on the electrode surface to expose their 5′ overhang and to hybridize with the DNA complexes linked to the gold nanoparticles (AuNPs). Consequently, large amounts of AuNPs, each loaded with a number of quadruplex DNA motifs, can be bound on the electrode surface and remarkably enhance the signal. Under optimal conditions, the method has a detection limit as low as 10 pg.mL^{-1} of CFP-10. The method was successfully applied to the diagnosis of *M. tuberculosis* in sputum.

Keywords *Mycobacterium tuberculosis* · Electrochemical method · Aptasensor · Dual amplification strategy · DNA click ligation · G-quadruplex-hemin complex · AuNPs · H_2O_2 · Hydroquinone · Azido group

Introduction

Mycobacterium tuberculosis (Mtb) remains one of the biggest health threats in the developing and some industrialized countries, of high rates of morbidity and mortality [1–4]. Therefore, establishing a sensitive, and highly efficient detection method for Mtb has always been an active area of research, with significant importance for human health. Currently, many diagnosis methods have been developed, such as mycobacterial culture, tuberculin skin test, and sputum smear microscopy method, but none of which are without their own problems [5–10]. For instance, the gold standard method for Mtb diagnosis is mycobacterial culture, which is often time consuming [11, 12]. Tuberculin skin test is the most widely used method, but it has low specificity [13–16]. While sputum smear microscopy method depends on both the quality and bacterial load of the sputum specimen and is of low sensitivity [17]. Over the past few years, although great efforts have been devoted to improve tuberculosis-detection methods, there is still an urgent need for an ultrasensitive, and efficient method for tuberculosis detection.

Jinlong Li and Kai Hu contributed equally to this work.

Electronic supplementary material The online version of this article (https://doi.org/10.1007/s00604-019-3780-3) contains supplementary material, which is available to authorized users.

✉ Jinlong Li
lijinlong1028@126.com

✉ Xia Zhang
zhangxia365@sina.com

[1] Department of Laboratory Medicine, the Second Hospital of Nanjing, Nanjing University of Chinese Medicine, Nanjing 210003, People's Republic of China

[2] Department of ophthalmology, the Nanjing Drum Tower Hospital, The Affiliated Hospital of Nanjing University Medical School, Nanjing 210004, People's Republic of China

[3] Department of Tuberculosis, the Second Hospital of Nanjing, Nanjing University of Chinese Medicine, Nanjing 210003, People's Republic of China

[4] Center for Global Health, School of Public Health, Nanjing Medical University, Nanjing 211166, People's Republic of China

Published online: 31 August 2019

To overcome the drawbacks of the traditional methods, many attempts have been made to use novel techniques such as the surface-plasmon resonance (SPR) [7, 11], and electrochemical method [18–21]. Among them, electrochemical methods exhibit unique merits of high sensitivity, which have attracted much attention in the field of disease diagnosis. However, most of the electrochemical methods for the assay of tuberculosis are based on one-way signal amplification strategy, which is not enough for the detection of low concentration biomarkers [22–25]. Since the level of tuberculosis antigen is very low, such as culture filtrate protein10 (CFP-10) protein, which is an early secretary antigen and used as an antigen for the detection of early tuberculosis (TB) infection. It is still highly required to develop amplification approaches, which may present more satisfactory results for tuberculosis assays.

Here, we have proposed a dual amplification strategy for CFP-10 detection based on DNA click ligation induced target cycling and G-quadruplex-hemin complex. This electrochemical method is not only the first report for CFP-10 antigen detection based on DNA nano-machinery, but it also has several advantages. (1) First, due to the specificity of aptamer toward CFP-10, this method demonstrates high selectivity. (2) Very low detection limit can be achieved due to the dual amplifications, which is conducive to the early diagnosis of tuberculosis. (3) The aptamer of CFP-10 lays the foundation for dual-signal amplification strategy and allows cost-efficient analysis as compared to the use of expensive antibodies. So, the strategy in this work may provide better performance in tuberculosis diagnosis.

Materials and methods

Materials

CFP-10 antigen and 6 kDa early secretory antigenic target (ESAT-6) antigen were obtained from Cusabio Co., Ltd. (https://www.cusabio.com/). CFP-10 ELISA kit was purchased from Jianglai Biotechnology Co., Ltd. (http://jianglai.foodmate.net/). H_2O_2, Bovine serum albumin (BSA), tris (2-carboxyethyl) phosphine hydrochloride (TCEP), hemin, EDTA, hydroquinone (HQ), and 6-mercapto-1-hexanol (MCH) were purchased from Sigma-Aldrich Chemical Co., Ltd. (https://www.sigmaaldrich.com/). Sputum samples were obtained from the Second Hospital of Nanjing. Other reagents used in this study were of analytical grade and used as purchased without further purification. Phosphate buffered saline (PBS; 0.1 M; pH 7.4) was prepared by dissolving 2.2 g Na_2HPO_4, 8.5 g NaCl, and 0.2 g NaH_2PO_4 in 1000 mL doubly distilled water. The buffer used in this work also included electrochemistry determination buffer (0.1 M PBS containing 0.2 mM HQ and 1.0 mM H_2O_2, pH 7.4), TE buffer (10 mM Tris-HCl and 1 mM EDTA, pH 7.4), and DNA immobilization buffer (10 mM Tris-HCl, 10 mM TCEP, 0.1 M NaCl and 1 mM EDTA, pH 7.4). Sample treatment solution was prepared by dissolving 4 g NaOH in 100 mL isopropanol. 12 sputum samples including 6 samples from tuberculosis patients and 6 samples from healthy volunteers were collected from the Department of Tuberculosis, the Second Hospital of Nanjing, which were approved by the ethical committees of the Second Hospital of Nanjing. Treatment of sputum samples: 1 mL sputum were added into 2 mL sample treatment solution, and incubated at room temperature for 10 min after severe shocks. The liquefied sputum solution was used to detect CFP-10. DNA Oligonucleotides (HPLC purified) used in this work were synthesized by Sangon Biotechnology Co., Ltd. (https://www.sangon.com/). And the sequences were listed as follows (from 5′ to 3′ end):

Dibenzocyclooctyne (DBCO)-DNA, SH-CGTACAACCAAC-DBCO;

CFP-10 aptamer (CFP-10 Apt) [26, 27],

*TCCTGAAAGGGGCCTGCCCCACTATCTCACATGGG*GTTCAGTTGGTTGTACG;

Complementary probe (CP) DNA,

TGAACCCCATGTGAGATAGTGGGGCAGGCCCCTTTCAGGA;

DNA 1, TGGGTAGGGCGGGTTGGGTTTTTT-SH;

DNA 2, GGGGCAGGCCCCTTTCAGGATTTTTT-SH;

and azido (N_3)-DNA, N_3-TGAACCCCATGTGAGATAGT.

The fraction of CFP-10 Apt written in italics can bind with CFP-10 antigen.

Preparation of AuNP-DNA complexes

AuNPs and AuNP-DNA complexes were prepared according to methods previously reported [28, 29]. Two different thiolated oligonucleotides (10 μM, 100 μL, molar ratio of DNA 1/DNA 2 = 1:10) were activated with TCEP (50 mM) for 2 h. Then the DNA solution was added into 1 mL AuNPs. After standing for 12 h with gentle shaking at 37 °C, 0.1% sodium dodecyl sulfate (SDS) was added into above system and the sodium chloride concentration was brought to 0.5 M. The solution was then centrifuged for 20 min at 12000 rpm and rinsed three times (10 mM PBS, pH 7.4) to remove the unbound DNA. The AuNP-DNA complexes were finally redispersed in 1 mL of PBS and stored at 4 °C for further use.

Electrochemical detection of CFP-10 (10-kDa culture filtrate protein) antigen

The gold electrode (3.0 mm in diameter) was prepared as in the previously report [30]. Then the gold electrode was incubated with oligonucleotides immobilization solution containing DBCO-DNA (1 μM) overnight, followed by treating with

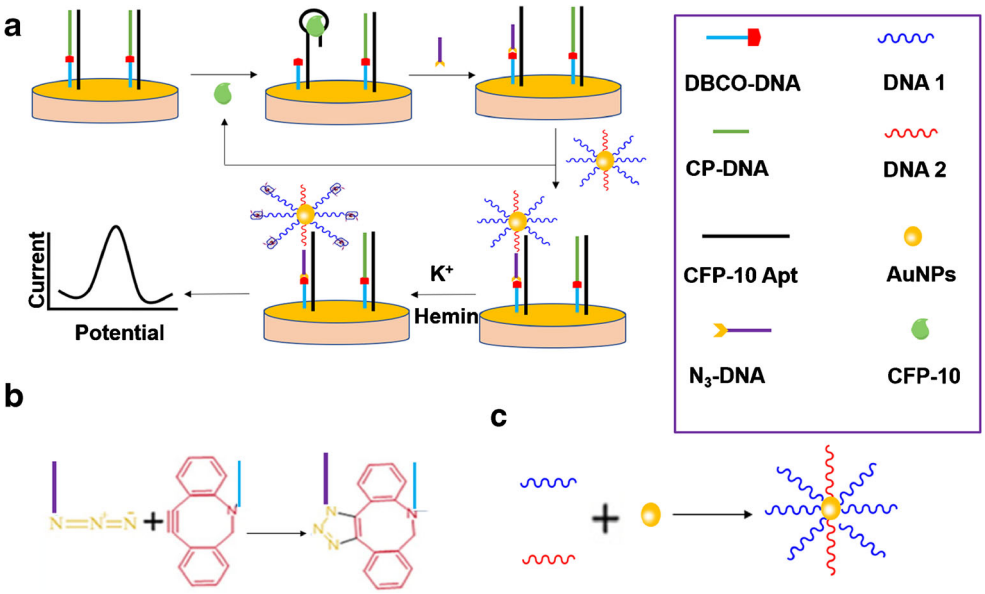

Scheme 1 Schematic illustration of the detection of CFP-10. **a** Detection procedure. **b** The reaction between DBCO-DNA and N_3-DNA. **c** The construction of AuNP-DNA complexes.

an aqueous solution of 1 mM MCH for 20 min to prevent non-specific adsorption. Then, the electrode was further rinsed with double-distilled water and dried again with nitrogen. Subsequently, the modified electrode was incubated with CFP-10 Apt (0.5 μM) and CP DNA (0.5 μM) for 1 h, followed by incubation with 0.25 μM N_3-DNA (dissolved in TE buffer, pH 7.4) mixed with different concentrations of CFP-10 antigen for 40 min at 37 °C. The electrode was incubated with 10 μL AuNP-DNA complexes at 37 °C for 1.5 h, Then, 10 μL hemin solution (25 mM HEPES, 50 mM KCl,

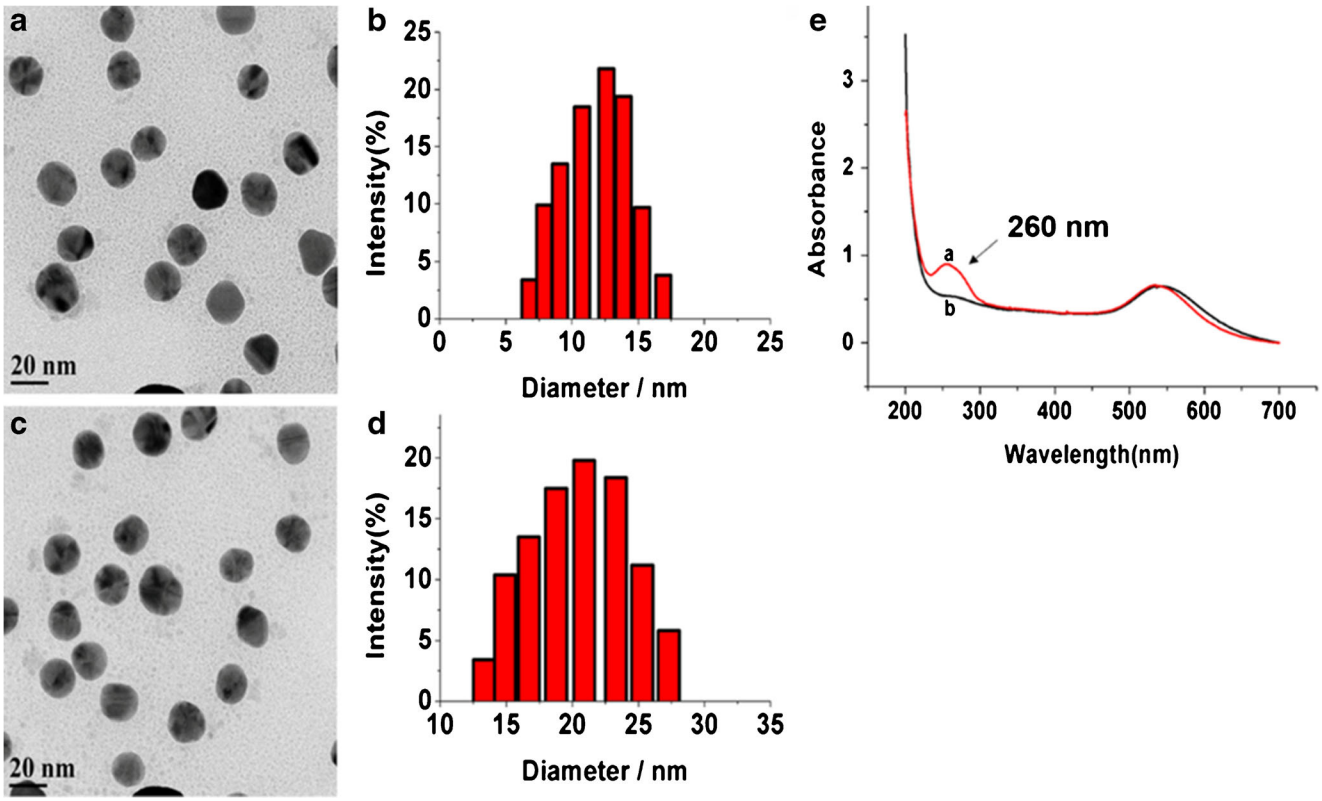

Fig. 1 **a** TEM image of the AuNPs, and the inset is the DLS size distribution of the AuNPs. **b** TEM image of AuNP−DNA complexes, ant the inset is the DLS size distribution of the AuNP−DNA complexes. (C) UV-vis spectra of (a) AuNPs, and (b) DNA/AuNPs

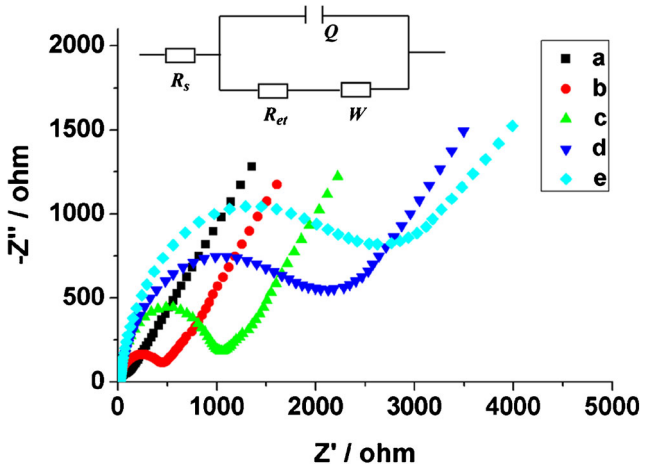

Fig. 2 Electrochemical impedance spectra of (a) the bare gold electrode, (b) the electrode treated with DBCO-DNA and MCH, (c) the electrode treated with CP DNA, and CFP-10 Apt. (d) the electrode treated with CP DNA, CFP-10 Apt, N_3-DNA, and AuNPs-DNA complexes, and (e) the electrode treated with CP DNA, CFP-10 Apt, CFP-10, N_3-DNA, and AuNPs-DNA complexes. Inset is the equivalent circuit. Rs, Ret, W and Q represent the solution resistance, the charge-transfer resistance, the warburg impedance and the constant phase element, respectively

200 mM NaCl, 12.5 mM $MgCl_2$) was added on the electrode surface at 37 °C for 2 h, followed by electrochemical measurements. Electrochemical measurements were carried out on 660D Electrochemical Analyzers with a conventional three electrode system, which is consisted of a saturated calomel electrode (SCE) as the reference electrode, a platinum wire as the counter electrode, and a gold electrode as the working electrode. Differential pulse voltammetry (DPV) was performed in electrochemistry determination buffer, while the electrochemical impedance spectra (EIS) experiments were performed in 5 mM $[Fe(CN)_6]^{3-/4-}$ with 1 M KNO_3. The experimental parameters were listed as follows: for DPV experiments, scan range, −0.1 V to 0.2 V; for EIS, bias potential, 0.213 V; amplitude, 5 mV; frequency range, 0.1 Hz to 100 kHz.

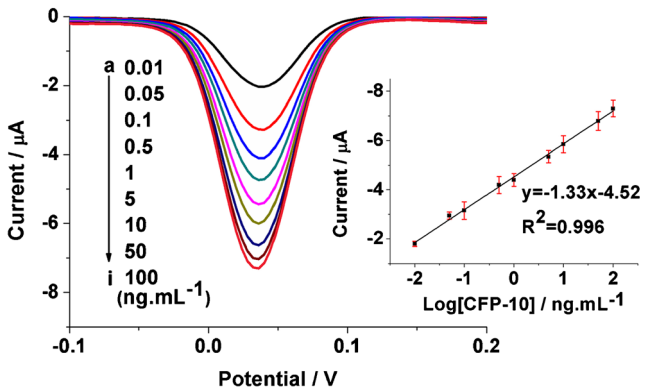

Fig. 3 DPV curves for different concentrations of CFP-10 (ng.mL^{-1}): (a) 0.01, (b) 0.05, (c) 0.1, (d) 0.5, (e) 1, (f) 5, (g) 10, (h) 50, and (i) 100 ng.mL^{-1} in 0.1 M PBS (pH 7.4) containing 1.0 mM H_2O_2 and 0.2 mM HQ. The inset is the calibration plot. Error bars indicate standard deviation of three independent experiments

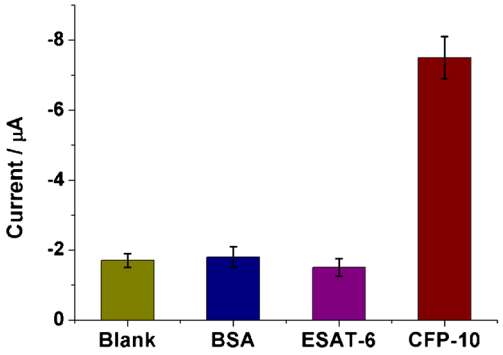

Fig. 4 Comparison of the DPV peak currents in the presence of BSA, ESAT-6, and CFP-10 respectively. All targets are at 100 ng.mL^{-1}. The error bars represent the standard deviation of three measurements. Blank control: 10 mM PBS (pH 7.4)

Enzyme-linked immunosorbent assay (ELISA) for CFP-10

These steps were carried out according to the instructions of CFP-10 kit.

Results and discussion

Method design

The principle of our design is illustrated in Scheme 1. CFP-10 Apt is first modified onto the electrode surface. In the presence of the CFP-10 antigen, which can bind to the aptamer (Apt) which will undergo a conformational change, releasing its complementary DNA that originally covers the upper portion of the Apt sequence. This can expose the DCBO group at the terminus of DCBO-modified DNA that still pairs with the stock of the Apt strand. The azide group of N_3-DNA can trigger the click chemical reaction smoothly. Subsequently, N_3-DNA shares the same complementary sequence as the released CP DNA, can bind with the CFP-10 Apt to liberate the antigen for the next cycle. This cycling of the target protein

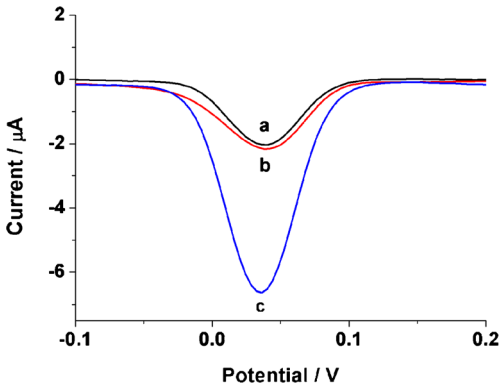

Fig. 5 DPVs obtained at the modified electrode incubated with biological samples. The sputum samples from (b) healthy volunteers, and (c) tuberculosis patients respectively. (a) Blank control: 10 mM PBS (pH 7.4)

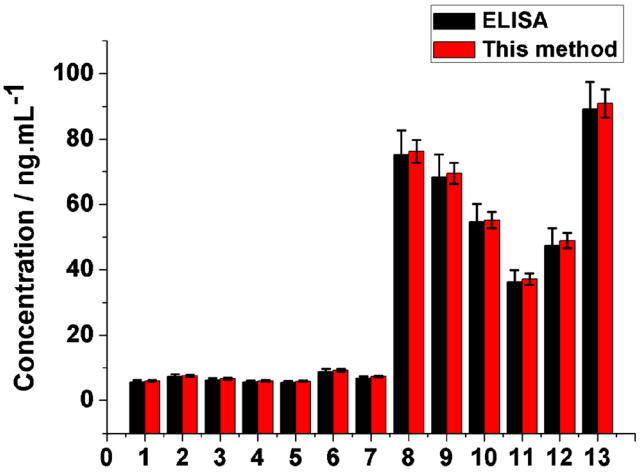

Fig. 6 The comparison between this method with ELISA. 1: Blank control: 10 mM PBS; 2–7: 6 sputum samples from healthy volunteers; 8–13: 6 sputum samples from tuberculosis patients. Error bars indicate standard deviation of three independent experiments

can be viewed as the first amplification step. Upon pairing with the N_3-DNA, the 5′ overhang of CFP-10 Apt become exposed and can hybridize with AuNPs-DNA complexes. After addition of hemin in the above system, G-quadruplex-based DNAzyme is formed due to the guanine-rich sequences of DNA 1. The G-quadruplex-hemin complex can catalyze the oxidation of hydroquinone by hydrogen peroxide to produce hydroquinone, which has a redox reaction on the surface of the electrode and produces a peak current, resulting the quantification of CFP-10. The signal of G- quadruplex-hemin complex and AuNPs occur at the same voltage in the presence of H_2O_2 and hydroquinone. And the signal of G-quadruplex-hemin complex is higher than AuNPs. Thus, the second amplification can be achieved mainly through the signal of G-quadruplex-hemin complex.

Characterization of AuNPs and AuNP-DNA complexes

Figure 1 a, b show the TEM images of the synthetic AuNPs and AuNPs−DNA respectively. The results show that AuNPs are monodispersed spherical particles, which have a narrow particle size distribution. And there is no obvious differences of morphology and dispersity between AuNPs and AuNP−DNA complexes. Dynamic light scattering (DLS) has been selected to analyze the hydrodynamic diameters of the AuNPs and AuNP−DNA complexes. As shown in the insets of Fig. 1a, b, the diameters of the AuNPs and AuNP−DNA complexes are about 12.6 and 20.4 nm, respectively. UV-vis spectrophotometry has been used to validate the modification of DNA to AuNPs. As shown in Fig. 1 c, compared with the UV-vis spectra of AuNPs (curve a), a strong absorbance peak at 260 nm can be detected for AuNP-DNA complexes, which shows an obvious change in the shape, position and symmetry of the absorption peak (curve b). The result demonstrates that AuNP-DNA complexes have been constructed successfully.

Characterization of the electrode modification

EIS has been selected to validate the modification processes of the electrode surface [31]. As shown in Fig. 2, the bare gold electrode displays as a straight line, suggesting the good electron transfer capability of electrode (curve a, 52 Ω). After incubation with DBCO-DNA and MCH sequently, a semicircle appears, meaning the DBCO-DNA and MCH are modified on the electrode, because the interfacial electron transfer resistance is increase (curve b, 478 Ω). After treatment with CP DNA and CFP-10 Apt sequently, the diameter of the semicircle increases again, meaning the binding of CFP-10 Apt with DBCO-DNA (curve c, 1264 Ω). Subsequently, treatment of the electrode with N_3-DNA and AuNP-DNA complexes does not change the impedance significantly, because AuNP-DNA complexes cannot bind with CFP-10 Apt in the absence of CFP-10 antigen (curve d, 2058 Ω). However, the diameter of the semicircle significantly increases in the presence of CFP-10 antigen due to the CFP-10 Apt binding with AuNP-DNA complexes (curve e, 2904 Ω).

Condition optimization

The following parameters are optimized: (a) the concentration of DBCO-DNA; (b) the concentration of CFP-10 Apt; (c) the ratio of DNA 1/DNA 2; (d) the pH of TE butter; (e) the incubation time; (f) the incubation time of hemin. The following

Table 1 A comparison of the method with previously reported ones

	Detection method	Linear Range	Detection limit	Assay times	References
1	Plasmonic ELISA	0–0.1 μg. mL^{-1}	0.01 μg. mL^{-1}	9.5 h	[32]
2	Surface plasmon resonance (SPR)	0.1–1 μg. mL^{-1}	100 ng. mL^{-1}	Not provided	[33]
3	Surface plasmon resonance (SPR)	0.1–150 ng. mL^{-1}	0.1 ng. mL^{-1}	2.5 h	[7]
4	Electrochemical	20–100 ng. mL^{-1}	15 ng. mL^{-1}	3 h	[18]
5	Electrochemical	0.01–100 ng. mL^{-1}	10 pg.mL^{-1}	5.5 h	This study

experimental conditions are found to give best results: (a) the concentration of DBCO-DNA is about 1.0 μM (Fig S1); (b) the concentration of CFP-10 Apt is about 0.5 μM (Fig S2); (c) the ratio of DNA 1/DNA 2 is about 1:10 (Fig S3); (d) the pH of the TE is about 7.4 (Fig S4); (e) the incubation time is about 40 min; (Fig S5); (f) the incubation time of hemin is about 2 h (Fig S6).

Electrochemical assay for the 10-kDa culture filtrate protein (CFP-10)

Under the optimized conditions, the concentration of CFP-10 antigen is investigated by DPV. As can be seen in Fig. 3, an increase of the electrochemical signal can be observed as the concentration of CFP-10 antigen increases from 10 pg.mL^{-1} to 100 ng.mL^{-1}. The linear relationship between the logarithm of CFP-10 antigen concentration and the electrochemical signal is obtained as $y = -1.33$ x-4.52, with a correlation coefficient of $R^2 = 0.996$. The detection limit is calculated to be 10 pg.mL^{-1} based on signal to noise ratio of 3 ($S/N = 3$), which is suitable for quantitative analysis of low-level tuberculosis antigen.

Selectivity of the electrochemical method

To test the selectivity of this electrochemical method, bovine serum albumin (BSA), and ESAT-6 have been selected as the interfere proteins for the assay. ESAT-6 is secreted by *Mycobacterium tuberculosis*, which is a low molecular weight protein and can be serve as a biomarker for early diagnosis of tuberculosis. As shown in Fig. 4, high peak current response can be obtained only for the samples containing the CFP-10 antigen. In the contrary, these control proteins will not produce significant electrochemical signal response. So, the dual amplification strategy can be used for the development of new method for selective detection of CFP-10 antigen.

Sputum sample analysis

To further explore the practical application of the sensing method for CFP-10 assay in complex sample, we have used this method to detect CFP-10 antigen in sputum samples of 6 TB patients and 6 healthy volunteers from the Second Hospital of Nanjing. As shown in Fig. 5, the CFP-10 antigen level of TB patients (curve c) is much high than healthy volunteers (curve b). To evaluate the reliability of the method, the assay results of CFP-10 antigen in sputum samples using the method are compared with the reference values obtained by ELISA. As shown in Fig. 6, the estimated values obtained by ELISA are nearly the same to our method, indicating an acceptable accuracy.

Conclusions

A dual amplification strategy for ultrasensitive detection of CFP-10 antigen has been established in this work through the DNA click ligation induced target cycling and gold nanoparticles loaded with G-quadruplex DNA motifs. The strategy may have several distinct advantages. First, this assay shows high selectivity toward CFP-10 antigen, because of the specificity of aptamer. Second, owing to the recycling target proteins and the G-quadruplex DNA motifs induced by clicking chemical reaction, the assay can achieve a lower detection limit toward CFP-10 antigen with 10 pg.mL^{-1} (Table 1). Third, using aptamer allows cost-efficient analysis compared to the use of antibodies. Considering the above advantages, the method for CFP-10 antigen assay based on the strategy proposed in this work might hold a great potential for further applications in biomedical research and clinical diagnosis in the future.

Acknowledgments The authors gratefully acknowledge the National Natural Science Foundation of China (Grant No. 81703088, and 81870695), the Medical Research Project of Jiangsu Provincial Health and Family Planning Commission, China (Grant No. H2018113), the Medical Science and Technology Development Foundation of Department of Health of Nanjing (YKK16107), and the Medical Science and Technology Foundation of Department of Health of Jiangsu Province (Grant No. Z2018034).

Compliance with ethical standards The author declares that there are no conflicts of interest.

References

1. Dheda K, Gumbo T, Gandhi NR, Murray M, Theron G, Udwadia Z, Migliori GB, Warren R (2014) Global control of tuberculosis: from extensively drug-resistant to untreatable tuberculosis. Lancet Respir Med 2(4):321–338
2. Sypabekova M, Bekmurzayeva A, Wang R, Li Y, Nogues C, Kanayeva D (2017) Selection, characterization, and application of DNA aptamers for detection of Mycobacterium tuberculosis secreted protein MPT64. Tuberculosis 104:70–78
3. Goletti D, Lee M-R, Wang J-Y, Walter N, Ottenhoff THM (2018) Update on tuberculosis biomarkers: from correlates of risk, to correlates of active disease and of cure from disease. Respirology 23(5):455–466. https://doi.org/10.1111/resp.13272
4. Floyd K, Glaziou P, Zumla A, Raviglione M (2018) The global tuberculosis epidemic and progress in care, prevention, and research: an overview in year 3 of the end TB era. Lancet Respir Med 6(4):299–314
5. Lei L, Liu Z, Zhang H, Yue W, Li CW, Yi C (2018) A point-of-need enzyme linked aptamer assay for Mycobacterium tuberculosis detection using a smartphone. Sensors Actuators B Chem 254:337–346
6. Liu W, Zou D, He X, Ao D, Su Y, Yang Z, Huang S, Zhao Q, Tang Y, Ma W (2018) Development and application of a rapidMycobacterium tuberculosisdetection technique using polymerase spiral reaction. Sci Rep 8(1):3003

7. Chen H, Liu F, Kwangnak L, Jaebeom Y, Zonghuang (2013) Sensitive detection of tuberculosis using nanoparticle-enhanced surface;plasmon resonance. Microchim Acta 180(5–6):431–436
8. Elsamadony H, Althani A, Tageldin MA, Azzazy HME (2017) Nanodiagnostics for tuberculosis detection. Expert Rev Mol Diagn 17(5):427–443
9. Kim J, Lee J, Lee KI, Park TJ, Kim HJ, Lee J (2013) Rapid monitoring of CFP-10 during culture of Mycobacterium tuberculosis by using a magnetophoretic immunoassay. Sensors Actuators B Chem 177(1):327–333
10. Troiano Araujo LDC, Wibrantz M, Rodriguez-Fernandez DE, Karp SG, Talevi AC, de Souza EM, Soccol CR, Thomaz-Soccol V (2019) Process parameters optimization to produce the recombinant protein CFP10 for the diagnosis of tuberculosis. Protein Expr Purif 154:118–125. https://doi.org/10.1016/j.pep.2018.09.016
11. Hong SC, Lee J, Shin HC, Kim CM, Park JY, Koh K, Kim HJ, Chang CL, Lee J (2011) Clinical immunosensing of tuberculosis CFP-10 in patient urine by surface plasmon resonance spectroscopy. Sensors Actuators B Chem 160(1):1434–1438
12. Makinen, J, Marjamaki, M, Marttila H, Soini H (2006) Evaluation of a novel strip test, GenoType Mycobacterium CM/AS, for species identification of mycobacterial cultures. Clin Microbiol Infect 12(5):481–483
13. Bai Y, Xue Y, Gao H, Wang L, Ding T, Bai W, Fan A, Zhang J, An Q, Xu Z (2008) Expression and purification of Mycobacterium tuberculosis ESAT-6 and MPT64 fusion protein and its immunoprophylactic potential in mouse model. Protein Expr Purif 59(2):189–196
14. Lambert L, Rajbhandary S, Qualls N, Budnick L, Catanzaro A, Cook S, Danielscuevas L, Reves EGR (2003) Costs of implementing and maintaining a tuberculin skin test program in hospitals and health departments. Infect Control Hosp Epidemiol 24(11):814–820
15. Sauzullo I, Massetti AP, Mengoni F, Rossi R, Lichtner M, Ajassa C, Vullo V, Mastroianni CM (2011) Influence of previous tuberculin skin test on serial IFN-Î³ release assays. Tuberculosis 91(4):322–326
16. Lee HJ, Choi HJ, Kim DR, Lee H, Jin JE, Kim YR, Lee MS, Cho SN, Kang YA (2016) Safety and efficacy of tuberculin skin testing with microneedle MicronJet600™ in healthy adults. Int J Tuberc Lung Dis 20(4):500–504
17. Sun J-R, Lee S-Y, Perng C-L, Lu J-J (2009) Detecting Mycobacterium tuberculosis in Bactec MGIT 960 cultures by Inhouse IS6110-based PCR assay in routine clinical practice. J Formos Med Assoc 108(2):119–125. https://doi.org/10.1016/s0929-6646(09)60042-5
18. Azmi UZM, Yusof NA, Kusnin N, Abdullah J, Suraiya S, Ong PS, Raston NHA, Abd Rahman SF, Fathil MFM (2018) Sandwich electrochemical Immunosensor for early detection of tuberculosis based on graphene/polyaniline-modified screen-printed gold electrode. Sensors 18(11). https://doi.org/10.3390/s18113926
19. He F, Xiong Y, Liu J, Tong F, Yan D (2016) Construction of au-IDE/CFP10-ESAT6 aptamer/DNA-AuNPs MSPQC for rapid detection of Mycobacterium tuberculosis. Biosens Bioelectron 77:799–804. https://doi.org/10.1016/j.bios.2015.10.054
20. Thakur H, Kaur N, Sareen D, Prabhakar N (2017) Electrochemical determination of M. tuberculosis antigen based on poly(3,4-ethylenedioxythiophene) and functionalized carbon nanotubes hybrid platform. Talanta 171:115–123
21. Torati SR, Reddy V, Yoon SS, Kim C (2016) Electrochemical biosensor for Mycobacterium tuberculosis DNA detection based on gold nanotubes array electrode platform. Biosens Bioelectron 78:483–488
22. Li J, Wang B, Gu S, Yang Y, Wang Z, Xiang Y (2017) Amperometric low potential aptasensor for the fucosylated Golgi protein 73, a marker for hepatocellular carcinoma. Microchim Acta 184(9):3131–3136. https://doi.org/10.1007/s00604-017-2334-9
23. Feng C, Wang Z, Chen T, Chen X, Mao D, Zhao J, Li G (2018) A dual-enzyme-assisted three-dimensional DNA walking machine using T4 polynucleotide kinase as activators and application in polynucleotide kinase assays. Anal Chem 90(4):2810–2815. https://doi.org/10.1021/acs.analchem.7b04924
24. Li J, Gao T, Gu S, Zhi J, Yang J, Li G (2017) An electrochemical biosensor for the assay of alpha-fetoprotein-L3 with practical applications. Biosens Bioelectron 87:352–357. https://doi.org/10.1016/j.bios.2016.08.071
25. Li C, Hu X, Lu J, Mao X, Xiang Y, Shu Y, Li G (2018) Design of DNA nanostructure-based interfacial probes for the electrochemical detection of nucleic acids directly in whole blood. Chem Sci 9(4):979–984. https://doi.org/10.1039/c7sc04663d
26. Zhanzhong MA, Yujiong W, Lianhua QIN, Yuansheng D, Qin XIE, Zhongyi HU (2008) Screening of aptamers to CFP-10 protein from Mycobacterium tuberculosis. Journal of Pathogen Biology 3(2):86–89
27. Tang X-L, Zhou Y-X, Wu S-M, Pan Q, Xia B, Zhang X-L (2014) CFP10 and ESAT6 aptamers as effective mycobacterial antigen diagnostic reagents. J Infect 69(6):569–580. https://doi.org/10.1016/j.jinf.2014.05.015
28. Zhang J, Liu Y, Lv J, Li G (2014) A colorimetric method for α-glucosidase activity assay and its inhibitor screening based on aggregation of gold nanoparticles induced by specific recognition between phenylenediboronic acid and 4-aminophenyl-α-d-glucopyranoside. Nano Res 8(3):920–930
29. Li J, He G, Wang B, Shi L, Gao T, Li G (2018) Fabrication of reusable electrochemical biosensor and its application for the assay of alpha-glucosidase activity. Anal Chim Acta 1026:140–146. https://doi.org/10.1016/j.aca.2018.04.015
30. Li J, He G, Mu C, Wang K, Xiang Y (2017) Assay of DNA methyltransferase 1 activity based on uracil-specific excision reagent digestion induced G-quadruplex formation. Anal Chim Acta 986:131–137. https://doi.org/10.1016/j.aca.2017.07.021
31. Yang D, Ning L, Gao T, Ye Z, Li G (2015) Enzyme-free dual amplification strategy for protein assay by coupling toehold-mediated DNA strand displacement reaction with hybridization chain reaction. Electrochem Commun 58:33–36. https://doi.org/10.1016/j.elecom.2015.06.001
32. Bakhori NM, Yusof NA, Abdullah J, Wasoh H, Noor SSM, Raston NHA, Mohammad F (2018) Immuno Nanosensor for the ultrasensitive naked eye detection of tuberculosis. Sensors 18(6). https://doi.org/10.3390/s18061932
33. Hong SC, Chen H, Lee J, Park H-K, Kim YS, Shin H-C, Kim C-M, Park TJ, Lee SJ, Koh K, Kim H-J, Chang CL, Lee J (2011) Ultrasensitive immunosensing of tuberculosis CFP-10 based on SPR spectroscopy. Sensors Actuators B Chem 156(1):271–275. https://doi.org/10.1016/j.snb.2011.04.032